IEEE Access
Multidisciplinary | Rapid Review | Open Access Journal

Received 5 February 2024, accepted 19 February 2024, date of publication 14 March 2024, date of current version 20 March 2024.

Digital Object Identifier 10.1109/ACCESS.2024.3375811

RESEARCH ARTICLE

Wideband Endfire Antenna Array for 5G mmWave Mobile Terminals

ALI ZIDOUR[1], MOULOUD AYAD[2], MOHAMMAD ALIBAKHSHIKENARI[3], (Member, IEEE), CHAN HWANG SEE[4], (Senior Member, IEEE), YING-XIN LAI[5], (Member, IEEE), YUE MA[6], BOUMEDIENE GUENAD[7], PATRIZIA LIVRERI[8], (Senior Member, IEEE), SALAHUDDIN KHAN[9], GIOVANNI PAU[10], (Senior Member, IEEE), AND TAYEB A. DENIDNI[11], (Fellow, IEEE)

[1]Department of Electrical Systems Engineering, Faculty of Technology, LIST Laboratory, M'hammed Bougara University, Boumerdes 35000, Algeria
[2]Department of Electronics, Faculty of Technology, Sétif1 University, Setif 19000, Algeria
[3]Department of Signal Theory and Communications, Universidad Carlos III de Madrid, Leganés, 28911 Madrid, Spain
[4]School of Computing, Engineering and the Built Environment, Edinburgh Napier University, EH10 5DT Edinburgh, U.K.
[5]School of Electronic Engineering and Intelligentization, Dongguan University of Technology, Dongguan 523808, China
[6]National Astronomical Observatories, Chinese Academy of Sciences, Beijing 100101, China
[7]Department of Electronics, Faculty of Technology, University of Hassiba Benbouali, Chlef 02000, Algeria
[8]Department of Engineering, University of Palermo, Palermo, 90128 Sicily, Italy
[9]College of Engineering, King Saud University, Riyadh 11421, Saudi Arabia
[10]Faculty of Engineering and Architecture, Kore University of Enna, 94100 Enna, Italy
[11]Institut National de la Recherche Scientifique, Université du Québec à Montréal, Montreal, QC H5A1K6, Canada

Corresponding authors: Giovanni Pau (giovanni.pau@unikore.it) and Mohammad Alibakhshikenari (mohammad.alibakhshikenari@uc3m.es)

Dr. Mohammad Alibakhshikenari acknowledges support from the CONEX-Plus programme funded by Universidad Carlos III de Madrid and the European Union's Horizon 2020 research and innovation programme under the Marie Sklodowska-Curie grant agreement No. 801538. This paper is also partially funded by British Council "2019 UK-China-BRI Countries Partnership Initiative" programme, with project titled "Adapting to Industry 4.0 oriented International Education and Research Collaboration". It is also supported by the Instrument and equipment function development project of Chinese Academy of Sciences. Besides above, the authors sincerely appreciate funding from Researchers Supporting Project number (RSP2024R58), King Saud University, Riyadh, Saudi Arabia.

ABSTRACT In this paper, a compact endfire antenna array with low-profile, small clearance, and wideband operation is proposed for millimeter-wave (mmWave) fifth-generation (5G) mobile terminals. The wideband operation is achieved by exciting two identical bow-tie dipoles inserted on both sides of a multilayer substrate fed by an asymmetric open-end stripline to slotline transition. The antenna performance is significantly improved by introducing a set of vertical metallic vias. The proposed antenna element can achieve 29 % from 24.2 GHz to 32.4 GHz with a peak realized gain that varies from 3.5 dBi to 4.5 dBi. A linear 4-element antenna array is arranged and fabricated to verify the proposed antenna beamforming capabilities. The simulated and measured bandwidth achieves a wide range of 34.4 % (24-34 GHz) to support 26, 28, and 30 GHz 5G mmWave bands with an isolation level better than 20 dB and a peak realized gain over the interested bands ranging from 7.56 to 8.14 dBi. The simulated array scanning angle is $\pm 68°$ at 28 GHz within 3-dB gain deterioration. Furthermore, the simulated spherical coverage has met the requirements of 3GPP standards which make the proposed antenna array a promising candidate to be integrated within mmWave 5G mobile devices.

INDEX TERMS 5G, antenna array, beamforming, endfire, mmWave bands, mobile terminal, wideband.

I. INTRODUCTION

Driven by stringent requirements for high data rates, low latency, and more reliable wireless systems. The advent of fifth-generation (5G) networks has revolutionized mobile functionalities and services to rely on always-on high-speed wireless connectivity. The millimeter wave (mmWave) spectrum with wider operating bandwidth has recently acquired research interest as enabling technology to unleash the full potential for next-generation mobile communication

The associate editor coordinating the review of this manuscript and approving it for publication was Mohammed Bait-Suwailam.

standards (beyond 5G) so as massive multiple-input multiple-output (MIMO) antenna systems [1], [2], [3], [4]. In order to compensate the inherent path loss and attenuation related to signal propagation over wireless mmWave channels and enhance beam coverage, beamforming antenna arrays with high gain and large scanning angle are prerequisites to be implemented in mmWave mobile terminals [5], [6], [7], [8].

From the vantage point of mobile terminals, a rudimentary approach integrates planar-shaped antennas with broadside radiation patterns, which limits the beamforming spherical range [9]. Therefore, endfire antennas are of particular relevance for link reliability due to their edge-positioning for large beam coverage, ease of integration within mobile PCB (printed circuit board), and their immunity against user impediment under practical scenarios [10], [11].

Recent studies have widely investigated antenna designs with endfire radiation for wideband mmWave operation including Vivaldi antennas, Metasurface antennas, printed Dipole antennas, and quasi-Yagi antennas. In [12], a Vivaldi antenna array operates in the band 24.6-28.5 GHz (14.7%). Metasurface-based antenna is proposed for endfire far-field and around 37 % (36.6-38.7 GHz) impedance matching and gain between 9.1-13.8 dBi are acquired [13]. In [14], a wideband log periodic dipole array antenna is designed to achieve endfire gain from 7.3 to 12.5 dBi over more than 31 % operating band. The mentioned antenna designs show promising bandwidth and high gain performance as low power and high data rate solution for mmWave applications. Yet with bulky radiating apertures make them unfeasible for mobile handsets. On the other hand, it's imperative to address the beam scanning angle for mmWave 5G beam coverage requirement [15]. In [16], Vivaldi antenna array operating at 28 GHz is able to provide ±60° beam coverage. In [17], a printed-dipole array element with endfire radiation is used to achieve a broadband operation bandwidth of 36.2% (26.5-38.2 GHz) and low isolation port (20 dB) with 0.52λ inter-element spacing using resonant stub decoupling structure (whereλ is the wavelength at the center frequency of the operating band). In [18], a quasi-Yagi array antenna with 180° scanning range via beam switching realizes a wide bandwidth of 42.5 % and gain of 8 dBi. However, a few low-profile endfire antenna arrays are compatible to accommodate the compactness tendency driven by recent design criteria that have imposed a very limited space to integrate mmWave antenna arrays since flagship handsets are excessively featuring full display panels and bigger batteries. Thereby, compact arrays with small ground clearance are required. Hence, the clearance on the ground plane reserved for antenna integration for efficient antenna functioning becomes a crucial factor in the design of 5G antennas. In addition, overall antenna dimensions and ease of integration with radio frequency integrated circuits (RFICs) must be notably considered to be fully integrated within mobile terminal's PCBs. The most interesting designs for small clearance have been presented in [19], a compact antenna array based on quasi-Yagi element operating in the band (25.9-30.25 GHz) with 0.23λ ground clearance. A quad-mode endfire phased antenna array with a reduced clearance of 0.15λ is designed to obtain a relative bandwidth of 27.6 % [20]. However, the operating bands are limited and still unmatched with the 5G NR bands. In [21], a quasi-Yagi antenna array with an entire ground plane is made with increasingly relative permittivity dielectric layers to shift the radiated beam towards the endfire direction via refraction and reflection and around 22.22 % impedance bandwidth is obtained. Yet with a relatively thick substrate (0.12λ).

According to the Third-Generation Partnership Project technical specification (3GPP TS 38.101-2 release 16.7.0), 5G new radio sub-mmWave spectrum allocations, denoted frequency range 2 (5G NR FR2), are selected [22]. The broadband range from 24.25 to 29.5 GHz (19.5%) is considered a pioneer 5G mmWave band. Thereby, wideband antenna designs with high gain and symmetric radiation patterns for beam scanning applications are needed. Such design specifications are very challenging for both academic research and industry. Thus, developing a design solution that can enhance the bandwidth with decent radiation and beam scanning performance while still maintaining a compact size, low profile and small ground clearance is indeed required and challenging.

Amid the aforementioned requirements, this paper proposes a compact endfire antenna array, which operates in the frequency bands of 26 GHz, 28 GHz, and 30 GHz for 5G NR mobile communication. The main features and highlights of the presented design are as follows:

1) The array is compact in size (19 mm), low profile (0.712 mm), and has a small clearance (1.9 mm).
2) The proposed array covers a wide bandwidth including lower operating frequencies (e.g., n258 band) in which the isolation level is below 20 dB for 4.7 mm inter-element spacing without any decoupling structure.
3) The phased array spans a wide beam scanning range of ± 68° at 28 GHz.

II. ANTENNA DESIGN

A. ANTENNA ELEMENT CONFIGURATION

The configuration of the proposed endfire antenna element is shown in Fig. 1. As illustrated in the perspective view, stacked substrate layers (Sub. 1 and Sub. 2) of Rogers RO4350B ($\epsilon_r = 3.66$, $tan\delta = 0.0037$) and prepreg layer (P.P) of Rogers RO4450F ($\epsilon_r = 3.52$, $tan\delta = 0.004$) in between as a bonding layer are used to construct the antenna PCB. The antenna element consists of two identical bow-tie-like dipoles as a main radiator joined to a truncated ground plane as a reflector were printed on both top and bottom sides of the antenna PCB, which are labelled as M1 and M3, respectively. The bow-tie dipole topology is modified to reduce the radiating structure for small clearance applications. The antenna feeding is realized by an integrated open-ended stripline balun (M2). The antenna unit radiating

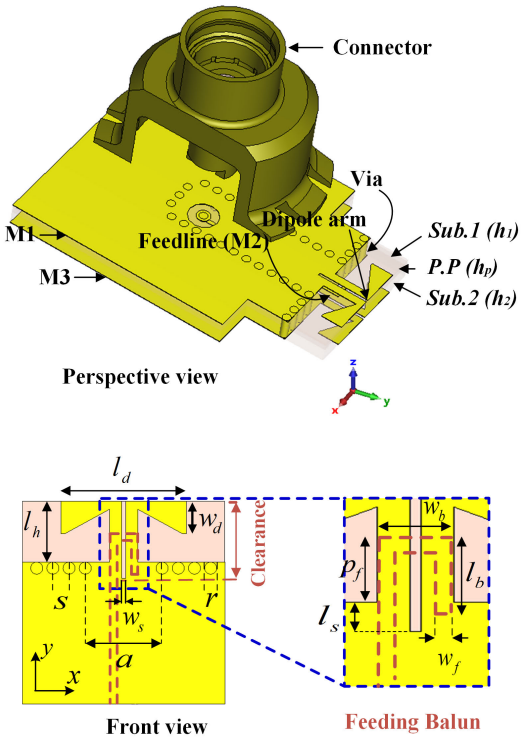

FIGURE 1. Configuration and dimension details of the antenna element. (Design parameters are: $l_d = 3.1$, $w_d = 0.8$, $l_h = 1.5$, $l_s = 0.4$, $w_s = 0.1$, $l_b = 0.8$, $w_b = 0.7$, $w_f = 0.15$, $p_f = 0.45$, $a = 2$, $s = 0.45$, $r = 0.15$, $h_1 = 0.1$, $h_2 = 0.51$, $h_p = 0.102$; All in mm).

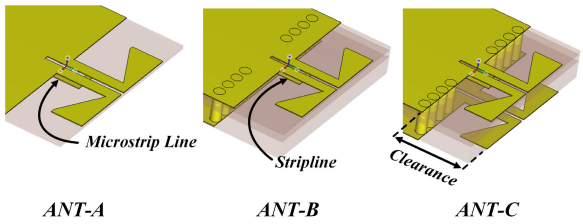

FIGURE 2. Steps evolution of the antenna design process.

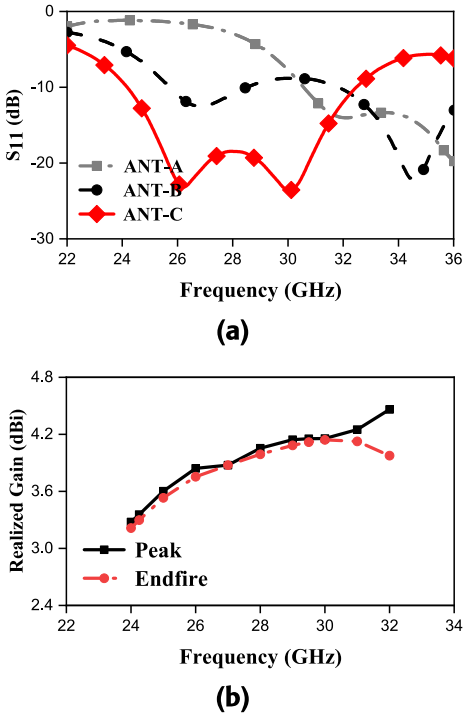

FIGURE 3. Simulated (a) reflection coefficients (b) realized gains of the antenna element.

structure has a very compact size of only 5 mm × 1.9 mm × 0.712 mm (0.56λ × 0.52λ × 0.057λ, where λ is the free-space wavelength of 24.25 GHz).

B. DESIGN PROCESS

The design process of the antenna element, as shown in Fig. 2 is described in detail to explain the operating principle. At the first stage, the single element (ANT-A) was designed on one substrate layer of a Rogers 4350B ($h_s =$ 0.1 mm, $\epsilon_r = 3.66$, $tan\delta = 0.0037$). The antenna comprised a printed bowtie-like dipole inserted to a truncated ground plane. The feeding structure that is etched on the opposite side of the substrate excite the dipole by a 50 Ω microstrip-line balun to slotline transition. Next, we propose in ANT-B an improved impedance matching approach with an open-end asymmetric stripline balun to excite the dipole. Stacked substrates are used to integrate the feeding structure. With a completed ground plane in (M3), the coupling between the dipole and the bottom ground would induce the impedance mismatch and deteriorate radiation efficiency. Therefore, a clearance below the dipole is required. The simulated reflection coefficients of ANT-A and ANT-B are shown in Fig. 3(a). It can be found that ANT- A and ANT-B have a common resonance range above 30 GHz. ANT-B has more resonances at frequencies below 30 GHz, which corresponds to the effect of the bottom layer. Compared with ANT-A, ANT-B has achieved a much wider bandwidth and enfold more lower operating frequencies while the size of the radiating structure was the same.

At the proposed setup (ANT-C), a pair of dipoles is inserted in both top and bottom metallic layers (M1, M3) to further enhance impedance matching and endfire radiation characteristics. A metallic vias are introduced between the two metallic layers as grounding pins to improve the impedance bandwidth and suppress the unwanted surface waves. The simulated reflection coefficient of ANT-C is also depicted in Fig. 3(a). A wide impedance bandwidth can be reached from 24.2 GHz to 32.4 (29 %).

As can be seen in Fig.3(b), ANT-C achieved good endfire performance in the *y*-axis direction. However, the radiation direction was tilted a bit at higher frequencies in the vertical plane (*yoz*) towards the broadside direction due to the effect of the driven bottom dipole resulting from the asymmetric feeding structure. The endfire gain was 3.9 dB compared to 4.5 dB of maximum realized gain at 32 GHz.

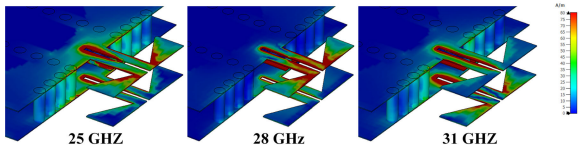

FIGURE 4. Simulated surface current distribution of the single antenna.

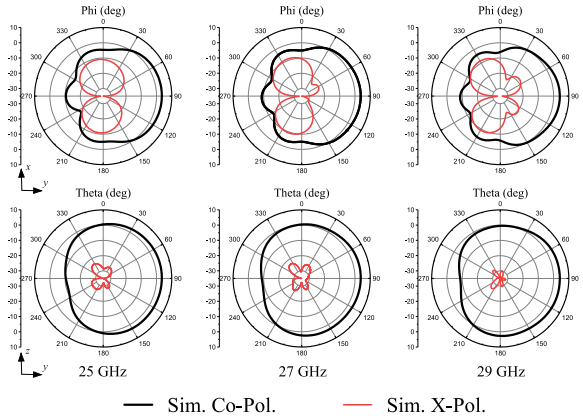

FIGURE 5. Radiation patterns of the antenna element at 25 GHz, 27 GHz, and 29 GHz; (Phi): horizontal plane (*xoy*), (theta): vertical plane (*yoz*).

To further reveal the operating mechanism of the proposed antenna. The surface currents on both top and bottom metallic planes (M1, M3) are shown in Fig. 4. The surface currents distribute conversely between top and bottom metallic planes. At the top metallic plane (M1), the surface current spread along the dipole and concentrates close to the notch for the resonant frequencies below 28 GHz. The currents become much stronger than the opposite plane which keeps endfire radiation pattern. Hence, the realized radiation pattern consists of the radiation from the electric current on the dipole arms and the magnetic current from the notch. At the bottom metallic plane (M3), stronger surface currents than the top at higher resonant frequencies. The currents concentrated around the inner slot and dipole arms. The magnetic current on the inner slot contributes effectively to generate the radiation pattern. Thus, the top plane of the antenna contributes to the radiation at lower resonant frequencies whereas the bottom plane contributes to the radiation at the higher ones. It's worth noting that the tilted radiation pattern at higher resonant frequencies is owing to the radiation of the bottom dipole. Otherwise, the inner slot is responsible of the cross-Pol part of the radiation pattern.

Fig. 5 shows the simulated radiation patterns of the optimized antenna in the vertical plane (*yoz*) and in the horizontal plane (*xoy*) at 25, 27, and 29 GHz. All are symmetric and have endfire radiation in the different operating bands. The realized gain is 3.6 dBi at 25 GHz and 4.15 dBi at 29 GHz. The cross-polarization level is at least 10 dB lower.

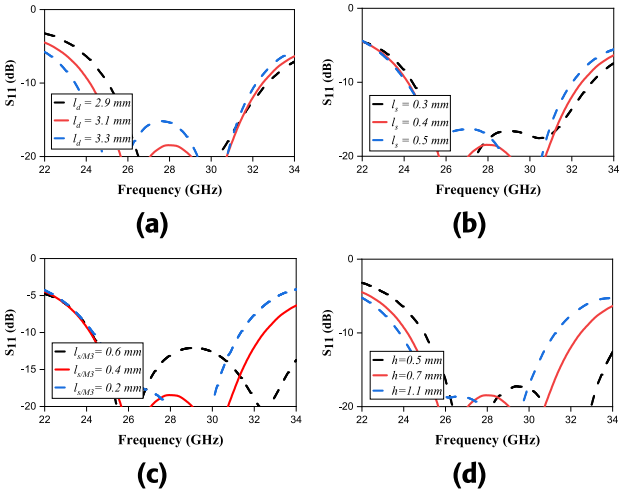

FIGURE 6. Reflection coefficients of the proposed antenna element. (a) l_d = varied (b) l_s = varied (c) $l_{s/M3}$ = varied (d) h = varied.

C. PARAMETRIC STUDY

The resonant frequencies of the proposed antenna element can be controlled by adjusting the critical parameters including the dipole length (l_d) and the inner slot length (l_s). According to Fig.6(a), the lower resonant frequency can be governed by tunning the bow tie arm's length (l_d) as the lower resonance shifts higher when the dipole arm (l_d) decreases. Otherwise, in Fig. 6(b), The higher resonance can be managed by changing the inner slot length (l_s) in the ground plane without affecting the lower resonance frequency. The higher resonances move further when (l_s) is shorter. Hence, a wide bandwidth can be attained when the two resonance frequencies are more parted. The tuning of the height of dipole arms (l_h) has a slight influence on the bandwidth but it can significantly influence the total gain of the antenna.

In the other hand, it's worth mentioning that the optimization of impedance bandwidth performance based on the parametric sweep can be done where only one parameter is tuned. Fig. 6(c) shows the reflection coefficient at different values of ($l_{s/M3}$). As seen, the parameter ($l_{s/M3} = 0.2$ mm) achieves an improved impedance bandwidth. It can be noticed that the optimized single antenna has a wide bandwidth potential, the tunning of the bottom ground slot can significantly enhance the bandwidth at the drawback of endfire gain deterioration. Therefore, quasi-endfire radiation may be considered for broad impedance bandwidth applications.

To investigate the influence of profile thickness on the impedance bandwidth of the proposed antenna, different profile values have been compared. By keeping (h_1) fixed, the total substrate thickness (h) impact on the impedance matching is plotted in Fig. 6(d). The impedance matching is enhanced with the decrease of (h) due to the effect of the bottom dipole. As (h) increases, the bandwidth becomes limited since the bottom dipole is barely excited. In the

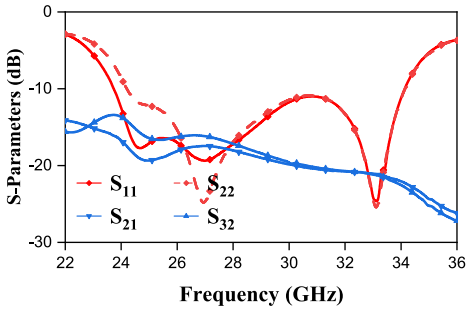

FIGURE 7. Simulated S-parameters of the array antenna elements.

proposed design, (h) is chosen to be 0.7 mm for a trade-off between the antenna performance and low-profile thickness.

III. ANTENNA ARRAY AND SIMULATION

To achieve high gain and beam scanning of beamforming capabilities, the proposed antenna element is expanded to a linear 1 × 4 antenna array. In this section, a mmWave array configuration featuring less than 0.07λ profile height has been designed with a typical spacing between the adjacent elements close to half-wavelength to be 4.7 mm (0.44λ at 28 GHz), to maintain port isolation for wide beam scanning range. The array radiating aperture becomes more compact with an overall dimensions of only 19 mm × 1.9 mm × 0.712 mm. The feeding power is provided via MMPX coaxial type connectors overlined on the top ground plane where the array element is excited by an open-end stripline connected to the inner connector through metal via. The surface wave suppression vias have been added around each feeding structure to reduce the power loss of the stripline.

A. BANDWIDTH AND RADIATION PERFORMANCE

The simulated S-parameters of the antenna array are depicted in Fig. 7. The achieved impedance matching with reflection coefficients in terms of −10 dB is 34.4 % from 24-34 GHz, which covers the mmWave 5G NR bands; n257 (26.50 - 29.50 GHz), n258 (24.25 - 27.50 GHz), n261 (27.5 - 28.35 GHz) [22]. The mutual coupling is below −15 dB, exhibiting a high level of port isolation over the operating band.

The radiation characteristics of the antenna array are presented in Fig. 8. The simulated 2D polar radiation patterns in (xoy) plane and (yoz) planes generated by array elements at 24 GHz, 26 GHz, 28 GHz, and 30 GHz are listed. Various frequencies were selected to address the lower, middle, and upper of interested bands. As illustrated, the antenna array has stable radiation patterns all over the addressed bands in both (xoy) and (yoz) planes. Also, as can be seen, the radiation patterns point to the $+y$ axis, which means that the antenna has endfire radiation. The simulated cross-polarization is much lower than co-polarization in both planes. The proposed array exhibits sufficient efficiencies over a wide operating bandwidth of more than −0.41 dB (90%) and −0.65 (86%) radiation and total efficiencies, respectively.

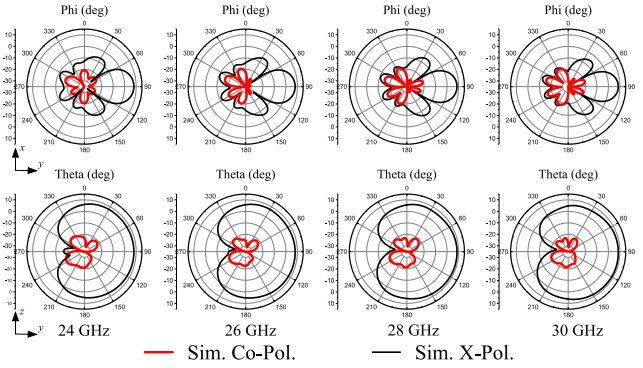

FIGURE 8. Simulated radiation patterns of the 4-element array antenna at 24 GHz, 26 GHz, 28 GHz, and 30 GHz.

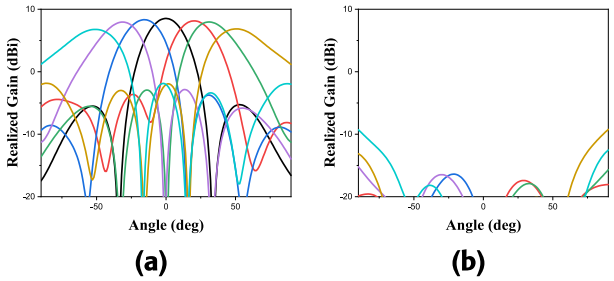

FIGURE 9. Simulated beam scanning patterns in the horizontal plane (*xoy*) at 28 GHz (a) Co-Pol. (b) X-Pol.

The beam scanning performance has been calculated in post processing based on the simulated radiation patterns of each element. The maximum realized gain of seven array beams is given at each angle of the horizontal plane to derive the scanning pattern. These beams were generated using equal magnitude and phase variance between adjacent feeding ports varies from −135° to +135° with progressive phase shift step ($\Delta\varphi$) of 45°. The cartesian beam scanning pattern at 28 GHz in the (xoy) plane is depicted in Fig. 9. With an average realized gain greater than 5.5 dBi, the phased array achieves a wide 3-dB beam scanning range of ±68°.

In order to investigate the influence of mobile devices (casing and metallic components) on the antenna array performance, the proposed array module is installed in a mobile device model, as shown in inset of Fig.10(a). The impedance matching and radiation patterns will be changed due to the different boundary conditions in the device model compared with free space (FS) [23]. As can be seen in Fig. 10(b), The installed array with clearance (labeled as W/C) achieves a broad bandwidth from 24 to 34 GHz for $|S_{11}| \leq$ −10 dB, which covers the 5G bands within (24.25 - 29.5 GHz). Besides, low mutual couplings have been obtained between the radiating elements. Furthermore, due to the degradation in radiation efficiency and impedance matching, it is very difficult to completely integrate densely packed dipole elements with a metallic shield nearby since dipole antenna performance is vulnerable to metallic components vicinity and more affected by full metallic display shield (zero

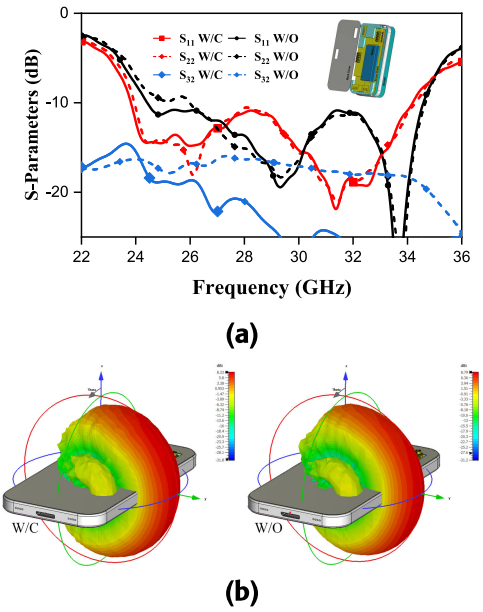

FIGURE 10. Simulation of the integrated antenna array. (a) S-parameters (b) 3D Radiation patterns of the installed array at 28 GHz.

TABLE 1. Realized gains of the array antenna at 28 GHz.

Realized Gain	Standalone	W/C	W/O
Simulated Endfire (dBi)	8.53	7.94	8.66
Simulated Peak (dBi)	8.56	8.23	8.79

clearance). In line with stringent requirements of antenna design for mobile terminals that impose a full metallic display shield, the influence of the shield has also been investigated. Considering the typical thickness of recent mobile devices (7-10 mm), the array is placed 4 mm apart from the metallic display shield (Labeled W/O). Nevertheless, as indicated in Fig. 10(a), the impedance matching still satisfies decent performance in terms of −10 dB (24.5 - 34.6 GHz).

Fig. 10(b) demonstrates the simulated 3D radiation patterns of the installed array at 28 GHz. As can be seen, the installed array achieves good endfire radiation, and the maximum co-polarization realized gain is 8.23 dBi at 28 GHz. In addition, the installed array with zero clearance can achieve greater gain (8.73 dB at 28 GHz). The cross-polarization slightly increases due to the effect of the surface current but is still acceptable.

As comparison, the realized gains at 28 GHz are summarized in Table 1. Both integrated array cases within the device operate effectively as in free space, which proves the compatibility of the proposed array with a realistic environment. The realized gains of the antenna array are convergent in the operating bands, indicating stable endfire radiation performance.

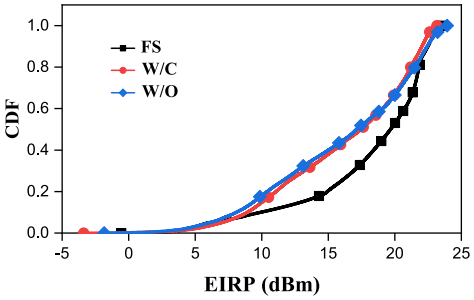

FIGURE 11. Spherical coverage of the proposed array at 28 GHz (The accepted power at each array element is set to be 9 dBm).

B. SPHERICAL COVERAGE

The coverage efficiency is a valuable ratio to determine the spherical coverage in terms of the total achievable gains at each possible solid angle from the threshold gain of beam scanning capability compared to the maximum solid angle. Moreover, in a wireless system, other factors influence the spherical coverage including the power sensitivity, transmission losses, and the insertion loss of the transceiver chain. Accordingly, spherical coverage in the case of mmWave 5G cellular devices is a critical performance metric to quantify the beam coverage ability to sustain the link budget regarding the line-of-sight (LoS) direction mismatching due to the randomly oriented mobile terminals [24]. The equivalent isotropically radiated power (EIRP) values at certain percentile of the cumulative distribution function (CDF) curve is defined to characterize the uplink spherical coverage. As a result, the spherical coverage of the proposed antenna array has also been calculated for both array standalone and installed into a handset model. The codebook of the array ports excitation for the accepted power magnitude is normalized to be 9 dBm for each antenna element based on progressive phase shift scheme. Four beams are used in each scenario to achieve the proposed array's spherical coverage. The EIRP is related to the simulated realized antenna gain. Fig. 11 depicts the spherical coverage of the proposed antenna array at 28 GHz. The simulation results show EIRP fading about 2.5 dB at CDF 50 % compared to the standalone case indicating the stricter effect of the device model. Nevertheless, The array coverage has met the power class 3 (PC 3) requirements of the handheld mobile devices for operating bands n257, n258, and n261 of minimum peak EIRP of 22.4 dBm at CDF of 100%, and 11.5 dBm at CDF of 50% [22].

IV. FABRICATION AND MEASUREMENTS

To validate and verify the accuracy of the simulation results, an array antenna prototype is fabricated and measured. The S-parameters were tested by VNA model: R&S ZVA40. The photographs of the fabricated array prototype and measurement setup are shown in Fig. 12.

Fig. 13 plots and compares the simulated and measured reflection coefficients (S_{ii}) and the mutual coupling between

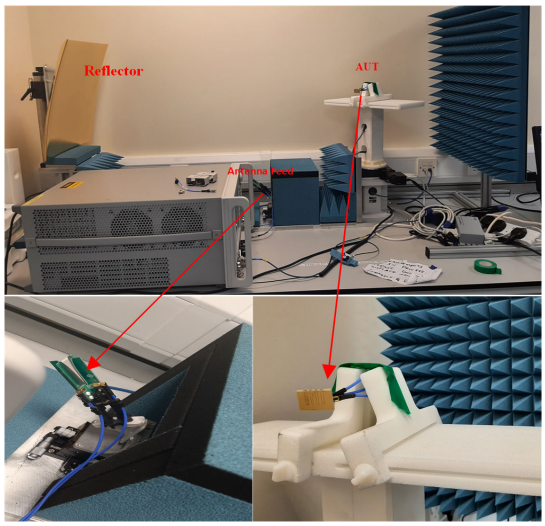

FIGURE 12. Photographs of the fabricated antenna array and far-field measurement setup.

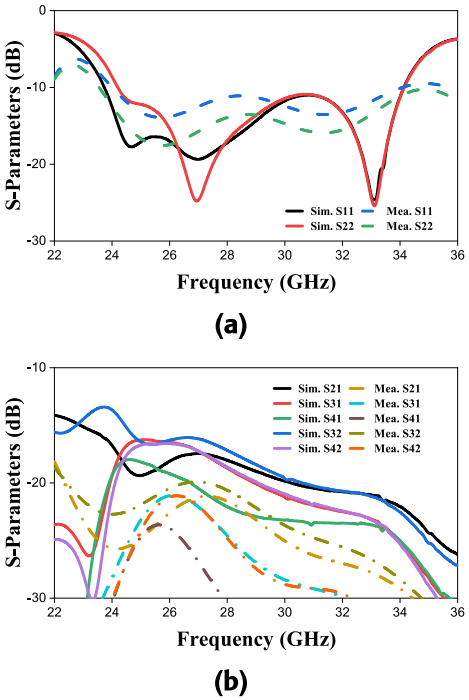

FIGURE 13. Simulated and measured S-parameters of the array antenna elements (a) Reflection coefficients (b) Mutual coupling.

the array elements (S_{ij}). The measured −10 dB operating band covers from 24 GHz to 34 GHz. As can be observed, a good agreement between simulation and measurement where the bandwidth obtained by simulation is very similar to the measured result. The measured mutual coupling between array elements is lower than 20 dB over the operating band while the simulated mutual coupling was lower than 15 dB.

Fig. 14 illustrates the simulated and measured 2D polar radiation patterns of the array element (port 2) in (*xoy*) plane

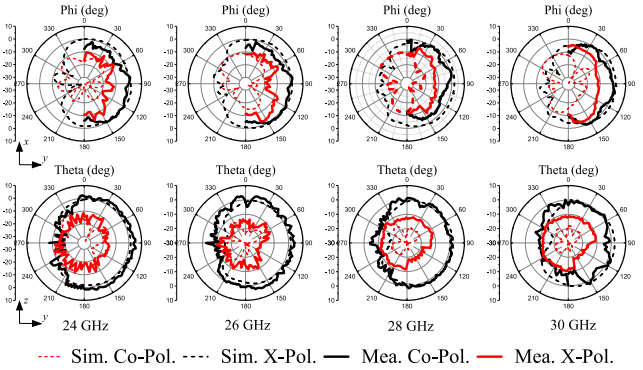

FIGURE 14. Simulated and measured radiation patterns of array port 2 at 24 GHz, 26 GHz, 28 GHz, and 30 GHz.

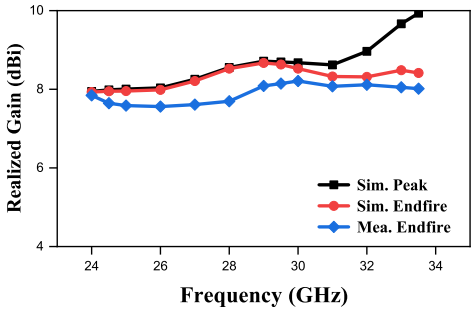

FIGURE 15. Simulated and measured realized gains versus operating bands of the antenna array at the endfire direction (+*y*).

(E-plane) and (*xoz*) plane (H-plane) at 24 GHz, 26 GHz, 28 GHz, and 30 GHz. As can be seen, a good agreement between the measured and simulated results are achieved particularly in the vertical plane. The proposed antenna array has a stable and symmetric endfire radiation patterns over the operating bands in both planes.

Fig. 15 plots the simulated and measured realized gains at +*y* direction versus operating frequencies. Within the interested bands from 24.25 to 29.5 GHz, the antenna array provides consistent endfire realized gain levels varying from 7.93 to 8.66 dBi and 7.56 to 8.14 dBi based on the simulated and measured results, respectively. Furthermore, based on the simulated results the peak realized gains are very close to the endfire realized gains. However, the endfire gain drop above 30 GHz is expected by simulation as discussed in section II.

To further investigate the proposed design, a comparison is carried out with other relevant mmWave endfire antenna arrays [13], [17], [18], [19], [20], [21], as listed in Table 2. The proposed antenna array has comprised the merits of compact size, small clearance and low profile, making it more suitable to be embedded into recent mobile devices. The bandwidth is larger than [19], [20], [21], reaching 34.4 % and much lower frequencies compared to wideband antenna arrays in [13], [17], and [18] to accommodate the entire frequency bands in the range (24.25-29.5 GHz) of 5G NR allocations. In addition, the proposed design provides the

TABLE 2. Comparison with other relevant endfire mmWave antenna arrays.

Ref.	Antenna Type	Array	Operating band (GHz)	BW (%)	Array Gain (dBi)	Scanning(°)	Element width (λ)	Profile (λ)	Clearance (λ)
[13]	SIW-fed Metasurface	1×4	26.6-38.7	37	9.1-13.8	N.M	0.16	0.16	0.82
[17]	Dipole	1×8	26.5-38	36.2	10-12	± 75	0.55	0.02	0.51
[18]	Quasi-Yagi	1×4	26-40	42.4	8	± 90	0.55	0.08	0.73
[19]	Quasi-Yagi	1×4	25.9-30.25	15.5	8.98-9.66	N.M	0.3	0.07	0.23
[20]	Dipole	1×8	25-33	27.6	≥ 12	± 70	0.36	0.15	0.13
[21]	Quasi-Yagi	1×4	24-30	22.2	6.64-8.15	± 54	0.32	0.12	0
Ours	Bow-tie Dipole	1×4	24-34	34.4	7.56-8.14	± 68	0.29	0.07	0.18

$BW = f_H - f_L/f_c$

lower inter-element spacing 4.7 mm with good isolation level and without any decoupling structure, which guarantees a larger scanning range. Compared to [19], the realized gain is a bit limited. However, it is qualified to reach the minimum acceptable value according to 3GPP regulation.

V. CONCLUSION

In this paper, a miniaturized, wideband endfire antenna phased array with a compact size, low-profile, and small ground clearance is proposed for 5G mobile applications. The array operates in a wide frequency range and has the ability to cover the bands within (24.25 - 29.5 GHz) frequency range with stable and decent performance in terms of radiation and efficiency for promising deployment of 5G mmWave bands to enable high data rates mobile communication. The pair of bow tie-like dipoles excited through slotline has a wide bandwidth potential offering a feasible solution for wideband mmWave antennas. In order to make the proposed antenna design more practical for the mobile terminal applications, the installed phased array was simulated in mobile device model and good radiation performance, wide frequency bandwidth, and spherical coverage make the presented antenna appropriate to meet the 5G mmWave requirements.

REFERENCES

[1] J. G. Andrews, S. Buzzi, W. Choi, S. V. Hanly, A. Lozano, A. C. K. Soong, and J. C. Zhang, "What will 5G be?" *IEEE J. Sel. Areas Commun.*, vol. 32, no. 6, pp. 1065–1082, Jun. 2014.

[2] M. Shafi, A. F. Molisch, P. J. Smith, T. Haustein, P. Zhu, P. De Silva, F. Tufvesson, A. Benjebbour, and G. Wunder, "5G: A tutorial overview of standards, trials, challenges, deployment, and practice," *IEEE J. Sel. Areas Commun.*, vol. 35, no. 6, pp. 1201–1221, Jun. 2017.

[3] M. Xiao, S. Mumtaz, Y. Huang, L. Dai, Y. Li, M. Matthaiou, G. K. Karagiannidis, E. Björnson, K. Yang, I. Chih-Lin, and A. Ghosh, "Millimeter wave communications for future mobile networks," *IEEE J. Sel. Areas Commun.*, vol. 35, no. 9, pp. 1909–1935, Sep. 2017.

[4] J. Lee, E. Tejedor, K. Ranta-aho, H. Wang, K.-T. Lee, E. Semaan, E. Mohyeldin, J. Song, C. Bergljung, and S. Jung, "Spectrum for 5G: Global status, challenges, and enabling technologies," *IEEE Commun. Mag.*, vol. 56, no. 3, pp. 12–18, Mar. 2018.

[5] I. A. Hemadeh, K. Satyanarayana, M. El-Hajjar, and L. Hanzo, "Millimeter-wave communications: Physical channel models, design considerations, antenna constructions, and link-budget," *IEEE Commun. Surveys Tuts.*, vol. 20, no. 2, pp. 870–913, 2nd Quart., 2018.

[6] W. Hong, K.-H. Baek, Y. Lee, Y. Kim, and S.-T. Ko, "Study and prototyping of practically large-scale mmWave antenna systems for 5G cellular devices," *IEEE Commun. Mag.*, vol. 52, no. 9, pp. 63–69, Sep. 2014.

[7] J. Helander, K. Zhao, Z. Ying, and D. Sjöberg, "Performance analysis of millimeter-wave phased array antennas in cellular handsets," *IEEE Antennas Wireless Propag. Lett.*, vol. 15, pp. 504–507, 2016.

[8] W. Roh, J.-Y. Seol, J. Park, B. Lee, J. Lee, Y. Kim, J. Cho, K. Cheun, and F. Aryanfar, "Millimeter-wave beamforming as an enabling technology for 5G cellular communications: Theoretical feasibility and prototype results," *IEEE Commun. Mag.*, vol. 52, no. 2, pp. 106–113, Feb. 2014.

[9] C.-X. Mao, S. Gao, and Y. Wang, "Broadband high-gain beam-scanning antenna array for millimeter-wave applications," *IEEE Trans. Antennas Propag.*, vol. 65, no. 9, pp. 4864–4868, Sep. 2017.

[10] W. Hong, K.-H. Baek, and S. Ko, "Millimeter-wave 5G antennas for smartphones: Overview and experimental demonstration," *IEEE Trans. Antennas Propag.*, vol. 65, no. 12, pp. 6250–6261, Dec. 2017.

[11] V. Raghavan, M.-L. Chi, M. A. Tassoudji, O. H. Koymen, and J. Li, "Antenna placement and performance tradeoffs with hand blockage in millimeter wave systems," *IEEE Trans. Commun.*, vol. 67, no. 4, pp. 3082–3096, Apr. 2019.

[12] S. Zhu, H. Liu, Z. Chen, and P. Wen, "A compact gain-enhanced Vivaldi antenna array with suppressed mutual coupling for 5G mmWave application," *IEEE Antennas Wireless Propag. Lett.*, vol. 17, pp. 776–779, 2018.

[13] T. Li and Z. N. Chen, "Wideband substrate-integrated waveguide-fed endfire metasurface antenna array," *IEEE Trans. Antennas Propag.*, vol. 66, no. 12, pp. 7032–7040, Dec. 2018.

[14] Q.-X. Chu, X.-R. Li, and M. Ye, "High-gain printed log-periodic dipole array antenna with parasitic cell for 5G communication," *IEEE Trans. Antennas Propag.*, vol. 65, no. 12, pp. 6338–6344, Dec. 2017.

[15] W. Hong, Z. H. Jiang, C. Yu, J. Zhou, P. Chen, Z. Yu, H. Zhang, B. Yang, X. Pang, M. Jiang, Y. Cheng, M. K. T. Al-Nuaimi, Y. Zhang, J. Chen, and S. He, "Multibeam antenna technologies for 5G wireless communications," *IEEE Trans. Antennas Propag.*, vol. 65, no. 12, pp. 6231–6249, Dec. 2017.

[16] W.-W. Lee, I.-J. Hwang, and B. Jang, "End-fire Vivaldi antenna array with wide fan-beam for 5G mobile handsets," *IEEE Access*, vol. 8, pp. 118299–118304, 2020.

[17] S. X. Ta, H. Choo, and I. Park, "Broadband printed-dipole antenna and its arrays for 5G applications," *IEEE Antennas Wireless Propag. Lett.*, vol. 16, pp. 2183–2186, 2017.

[18] C. Di Paola, S. Zhang, K. Zhao, Z. Ying, T. Bolin, and G. F. Pedersen, "Wideband beam-switchable 28 GHz quasi-yagi array for mobile devices," *IEEE Trans. Antennas Propag.*, vol. 67, no. 11, pp. 6870–6882, Nov. 2019.

[19] I.-J. Hwang, B. Ahn, S.-C. Chae, J.-W. Yu, and W.-W. Lee, "Quasi-yagi antenna array with modified folded dipole driver for mmWave 5G cellular devices," *IEEE Antennas Wireless Propag. Lett.*, vol. 18, pp. 971–975, 2019.
[20] I. Syrytsin, S. Zhang, G. F. Pedersen, and A. S. Morris, "Compact quad-mode planar phased array with wideband for 5G mobile terminals," *IEEE Trans. Antennas Propag.*, vol. 66, no. 9, pp. 4648–4657, Sep. 2018.
[21] Y. Liu, C. Zhao, Z. Yue, A. Ren, and Y. Jia, "A horizontally polarized end-fire antenna with complete ground for 5G mmWave applications," *Microw. Opt. Technol. Lett.*, vol. 62, no. 12, pp. 3936–3944, Dec. 2020.
[22] *User Equipment (UE) Radio Transmission and Reception—Part 2: Range 2 Standalone (Release 16)*, document TS 38.101-2, Version 16.7.0, Apr. 2021.
[23] W. Hong, "Solving the 5G mobile antenna puzzle: Assessing future directions for the 5G mobile antenna paradigm shift," *IEEE Microw. Mag.*, vol. 18, no. 7, pp. 86–102, Nov. 2017.
[24] K. Zhao, S. Zhang, Z. Ho, O. Zander, T. Bolin, Z. Ying, and G. F. Pedersen, "Spherical coverage characterization of 5G millimeter wave user equipment with 3GPP specifications," *IEEE Access*, vol. 7, pp. 4442–4452, 2019.

ALI ZIDOUR was born in Ouled Ben Abdelkader, Chlef, Algeria, in October 1988. He received the master's degree in telecommunication engineering from the University of Hassiba Benbouali, Chlef, in July 2015. He is currently pursuing the Ph.D. degree with the LIST Laboratory, Department of Electrical Systems Engineering, Faculty of Technology, M'hammed Bougara University, Boumerdes, Algeria. His research interests include electromagnetic systems, antennas and propagation, multiple-input multiple output (MIMO) antenna systems, substrate integrated waveguides (SIWs), impedance matching circuits, microwave and millimeter-waves antennas, and gap waveguide technology.

MOULOUD AYAD received the Engineering, Magister, and Ph.D. degrees in electronics from Sétif1 University, Algeria, in 2001, 2005, and 2015, respectively. He is currently an Assistant Professor with the Department of Electronics, Sétif1 University. He is also a member of the LPM3E Laboratory, University of Bouira, Algeria. His research interests include signal processing, microwave circuit design, microstrip, and waveguide structures.

MOHAMMAD ALIBAKHSHIKENARI (Member, IEEE) was born in Mazandaran, Iran, in February 1988. He received the Ph.D. degree (Hons.) with European Label in electronics engineering from the University of Rome "Tor Vergata," Italy, in February 2020. From May 2018 to December 2018, he was a Ph.D. Visiting Researcher with the Chalmers University of Technology, Gothenburg, Sweden. His training during this Ph.D. research visit included a research stage with Swedish Company Gap Waves AB, Gothenburg. Since July 2021, he has been with the Department of Signal Theory and Communications, Universidad Carlos III de Madrid (uc3m), Spain, as a Principal Investigator of the CONnecting EXcellence (CONEX)-Plus Talent Training Program and Marie Skłodowska-Curie Actions. He was also a Lecturer of the Electromagnetic Fields and Electromagnetic Laboratory, Department of Signal Theory and Communications, from 2021 to 2022, and he received the "Teaching Excellent Acknowledgement" Certificate for the course of electromagnetic fields from Vice-Rector of studies of uc3m. From December 2022 to May 2023, he spent three industrial and academic research visits with SARAS Technology Ltd. Company, Leeds, England; Edinburgh Napier University, Edinburgh, Scotland; and University of Bradford, West Yorkshire, England, which were defined by CONEX-Plus Talent Training Program and Marie Skłodowska-Curie Actions as his secondment research visit plans. His research interests include electromagnetic systems, antennas and wave-propagations, metamaterials and metasurfaces, sensors, synthetic aperture radars (SAR), 5G and beyond wireless communications, multiple input multiple output (MIMO) systems, RFID tag antennas, substrate integrated waveguides (SIWs), impedance matching circuits, microwave components, millimeter-waves and terahertz integrated circuits, gap waveguide technology, beamforming matrix, and reconfigurable intelligent surfaces (RIS), which led to achieve more than 5500 citations and H-index above 46 reported by Scopus, Google Scholar, and ResearchGate. He was a recipient of the three years Principal Investigator research grant funded by Universidad Carlos III de Madrid and the European Union's Horizon 2020 Research and Innovation Program under the Marie Skłodowska-Curie Grant started, in July 2021; the two years postdoctoral research grant funded by the University of Rome "Tor Vergata" started, in November 2019; the three years Ph.D. Scholarship funded by the University of Rome "Tor Vergata" started, in November 2016; and the two Young Engineer Awards of the 47th and 48th European Microwave Conference were held in Nuremberg, Germany, in 2017, and in Madrid, Spain, in 2018, respectively. In April 2020, his research article titled "High-Gain Metasurface in Polyimide On-Chip Antenna Based on CRLH-TL for Sub Terahertz Integrated Circuits" published in Scientific Reports was awarded as the Best Month Paper at the University of Bradford, West Yorkshire, England. He is serving as an Associate Editor for *Radio Science* and *IET Journal of Engineering*. He also acts as a referee in several highly reputed journals and international conferences.

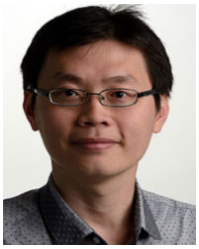

CHAN HWANG SEE (Senior Member, IEEE) received the B.Eng. degree (Hons.) in electronic, telecommunication and computer engineering and the Ph.D. degree from the University of Bradford, U.K., in 2002 and 2007, respectively. He is currently an Associate Professor with the School of Computing, Engineering and the Built Environment, Edinburgh Napier University, U.K., where he was the Head of Electrical Engineering and Mathematics, from 2019 to 2022. His research interests include wireless sensor network system design, computational bioelectromagnetics, antennas, microwave circuits, the Internet of Things (IoTs), microwave sensors, wireless power transfer, and acoustic sensor design. He has published over 250 peer-reviewed journal articles and conference papers in these research areas. He is the coauthor for one book and three book chapters. He was awarded a IEEE Malaysia AP/MTT/EMC Joint Chapter Best Paper Award, in 2020. He was a recipient of two Young Scientist Awards from the International Union of Radio Science (URSI) and Asia–Pacific Radio Science Conference (AP-RASC), in 2008 and 2010, respectively. He was awarded a certificate of excellence for his successful Knowledge Transfer Partnership (KTP) with Yorkshire Water on the design and implementation of a wireless sensor system for sewerage infrastructure monitoring, in 2009. He is a Chartered Engineer and a fellow of the Institution of Engineering and Technology. He is also a fellow of the Higher Education Academy, a full member of the EPSRC Review College, an Associate Editor of IEEE Access, and an Editor of *Journal of Electronics and Electrical Engineering*, *Scientific Reports*, *PeerJ Computer Science*, *PLOS One*, and *Wireless Power Transfer* journals. According to Web of Science, he has completed over 500 verified reviews and over 250 verified editor records.

YING-XIN LAI (Member, IEEE) received the B.S. and Ph.D. degrees from Southwest Jiaotong University (SWJTU), Chengdu, China, in July 2003 and December 2008, respectively. He is currently an Associate Professor with the School of Electronic Engineering and Intelligentization, Dongguan University of Technology (DGUT), Dongguan, China. His research interests include high-power microwave sources, antennas, millimeter passive devices, and microwave-photonic sensors.

YUE MA was born in Tangshan, Hebei, China, in 1986. She received the bachelor's and master's degrees (Hons.) in electrical and electronic engineering from the University of Bradford, U.K., in 2009 and 2010, respectively, and the Ph.D. degree from the University of Chinese Academy of Sciences with astronomical techniques and methods, in 2022. Her research field covers the mobile and satellite communication antenna studies that includes RFID passive tag design at Europe UHF band, MIMO mobile handset antenna designs, CPW, UWB, phased array antennas for wireless communication applications in U.K. Since 2013, she has been working at the development on wide band single pixel feed, phased array feed, low noise amplifier, filter designs for the square kilometer array (SKA) radio telescope, and the 500-meter Aperture Spherical Radio Telescope (FAST) with National Astronomical Observatories, Chinese Academy of Sciences. In 2017, she got Young Scientists Award in the 32nd International Union of Radio Science General Assembly and Scientific Symposium (URSI 2017 GASS).

BOUMEDIENE GUENAD received the magister degree in signals and systems and the Ph.D. degree in telecommunications science from the University of Tlemcen, Tlemcen, Algeria, in 2005 and 2013, respectively. He is currently an Assistant Professor with the Department of Electronics, Faculty of Technology, University of Hassiba Benbouali, Chlef, Algeria, and a Research Member with the Telecommunications Laboratory of Tlemcen (LTT), Tlemcen. His current research interests include multi-beam antenna arrays, fractal antennas, ultra-wideband antennas, and metamaterial antennas.

PATRIZIA LIVRERI (Senior Member, IEEE) received the "Laurea" degree (Hons.) in electronics engineering and the Ph.D. degree in electronics and communications engineering from the University of Palermo, Italy, in 1986 and 1992, respectively. She is currently a Professor with the Department of Engineering, University of Palermo, and a Visiting Professor with the San Diego State University. From 1993 to 1994, she was a Researcher with CNR. Since 1995, she has been serving as the Scientific Director for the Microwave Instruments and Measurements Laboratory, Engineering Department, University of Palermo. In 2020, she also joined the CNIT National Laboratory for Radar and Surveillance Systems RaSS, Pisa. Her research interests include microwave and millimeter vacuum high power (TWT, Klystron) and solid-state power amplifiers for radar applications; high power microwave source (virtual cathode oscillator, magnetically insulated transmission line oscillator); microwave and optical antennas, radar, and microwave quantum radar. She is the Principal Investigator of the Microwave Quantum Radar Project, funded by the Ministry of Defense, in 2021. She is the Supervisor of many funded project and the author of more than 200 published articles.

SALAHUDDIN KHAN, photograph and biography not available at the time of publication.

GIOVANNI PAU (Senior Member, IEEE) received the bachelor's degree in telematic engineering from the University of Catania, Italy, and the master's degree (cum laude) in telematic engineering and the Ph.D. degree from the Kore University of Enna, Italy. He is currently an Associate Professor with the Faculty of Engineering and Architecture, Kore University of Enna. He is the author/coauthor of more than 80 refereed articles published in journals and conference proceedings. He is a member of the IEEE (Italy Section) and he has been involved in several international conferences as the session co-chair and a technical program committee member. He serves/served as a leading guest editor in special issues of several international journals. He is an Editorial Board Member as an Associate Editor of several journals, such as IEEE Access, *Wireless Networks* (Springer), *EURASIP Journal on Wireless Communications and Networking* (Springer), *Wireless Communications and Mobile Computing* (Hindawi), *Sensors* (MDPI), and *Future Internet* (MDPI). His research interests include wireless sensor networks, fuzzy logic controllers, intelligent transportation systems, the Internet of Things, smart homes, and network security.

TAYEB A. DENIDNI (Fellow, IEEE) received the M.Sc. and Ph.D. degrees in electrical engineering from Laval University, Quebec City, QC, Canada, in 1990 and 1994, respectively. From 1994 to 2000, he was a Professor with Engineering Department, Université du Québec à Rimouski, Rimouski, QC, where he founded the Telecommunications Laboratory. Since August 2000, he has been with Institut National de la Recherche Scientifique (INRS), Université du Québec à Montréal, Montreal, QC. He founded the RF Laboratory, INRS-EMT, Montreal. He has a great experience with antenna design and he is leading a large research group consisting of three research scientists, six Ph.D. students, and one M.Sc. student. He served as a Principal Investigator on many research projects sponsored by NSERC, FCI, and numerous industries. His current research interests include reconfigurable antennas using EBG and FSS structures, dielectric resonator antennas, metamaterial antennas, adaptive arrays, switched multibeam antenna arrays, ultra-wideband antennas, and microwave and development for wireless communications systems. He was an Associate Editor of IEEE Antennas Wireless Propagation Letters, from 2005 to 2007, and IEEE Transactions on Antennas Propagation, from 2008 to 2010. Since November 2015, he has been an Associate Editor of *Electronics Letters* (IET). In 2012 and 2013, he was a recipient of INRS for outstanding research and teaching achievements.

Open Access funding provided by 'Università degli Studi di Enna "KORE"' within the CRUI CARE Agreement